NEW TRENDS IN FLUID MECHANICS RESEARCH
Proceedings of the Fifth International Conference on Fluid Mechanics, *Aug.15-19, 2007, Shanghai, China*

Receptivity to Free-stream Disturbance Waves for Blunt Cone Axial Symmetry Hypersonic Boundary Layer

Y. D. Zhang[1,2*], D. X. Fu[1], Y. W. Ma[1] , X. L. Li[1]

[1] *LNM, Institute of Mechanics, CAS, Beijing 100080, China*
[2] *China Academy of Aerospace Aerodynamics, Beijing 100074, China*
Email: zyd701@sina.com.cn

Abstract Based on high-order compact upwind scheme, a high-order shock-fitting finite difference scheme is studied to simulate the generation of boundary layer disturbance waves due to free-stream waves. Both steady and unsteady flow solutions of the receptivity problem are obtained by resolving the full Navier-Stokes equations. The interactions of bow-shock and free-stream disturbance are researched. Direct numerical simulation (DNS) of receptivity to free-stream disturbances for blunt cone hypersonic boundary layers is performed.

Key words: receptivity, shock-fitting, compact upwind scheme, DNS, blunt cone

INTRODUCTION

The laminar–turbulent transition process is a result of the nonlinear response of boundary layers to forcing disturbances.Receptivity, which is the process of environmental disturbances initially entering the boundary layers, is the first stage of laminar–turbulent transition. DNS is an important method to study the receptivity at high Mach number[1 - 3].In this paper, a high-order-accurate shock-fitting finite difference scheme is studied, which is based on fifth-order upwind compact schemes, sixth-order central schemes and third-order Runge-Kutta schemes. The receptivity of hypersonic boundary layers over a blunt cone is simulated.

Numerical method

1. Governing equations The governing equations are the unsteady Navier-Stokes equations. The bow shock is treated as a computational boundary, where the transient shock movement is solved as a part of the solutions.

2. Rankine-Hugoniot conditions The flow variables across the shock are governed by the Rankine-Hugoniot conditions, and the jump conditions for flow variables behind the shock are:

$$\begin{aligned} &\rho_1 (\boldsymbol{v_1} \cdot \boldsymbol{n} - z) = \rho_2 (\boldsymbol{v_2} \cdot \boldsymbol{n} - z) \\ &p_1 \boldsymbol{n} + \rho_1 \boldsymbol{v_1} (\boldsymbol{v_1} \cdot \boldsymbol{n} - z) = p_2 \boldsymbol{n} + \rho_2 \boldsymbol{v_2} (\boldsymbol{v_2} \cdot \boldsymbol{n} - z) \\ &\rho_1 E_1 (\boldsymbol{v_1} \cdot \boldsymbol{n} - z) + p_1 \boldsymbol{v_1} \cdot \boldsymbol{n} = \rho_2 E_2 (\boldsymbol{v_2} \cdot \boldsymbol{n} - z) + p_2 \boldsymbol{v_2} \cdot \boldsymbol{n} \end{aligned} \tag{1}$$

where p is pressure, ρ is density,$\boldsymbol{v}$ is the velocity vector,z is the normal velocity of shock,$\boldsymbol{n}$ is the normal vector of shock, the subscript 2 represent the variable immediately behind the shock and subscript 1 represents the variables on the free stream side of the shock surface.

3. Characteristic compatibility equations The unsteady Navier-Stokes equations in the computational domain immediately behind the shock can be written as

$$\frac{\partial \boldsymbol{U}}{\partial \tau}+\left(\frac{\partial \boldsymbol{E}}{\partial \boldsymbol{U}}\eta_x+\frac{\partial \boldsymbol{F}}{\partial \boldsymbol{U}}\eta_y+\eta_t\right)\frac{\partial \boldsymbol{U}}{\partial \eta}+\frac{\partial \boldsymbol{E}}{\partial \xi}\xi_x+\frac{\partial \boldsymbol{F}}{\partial \xi}\xi_y+\frac{\partial \boldsymbol{U}}{\partial \xi}\xi_t+\frac{\partial \boldsymbol{E}_v}{\partial \xi}\xi_x+\frac{\partial \boldsymbol{E}_v}{\partial \eta}\eta_x+\frac{\partial \boldsymbol{F}_v}{\partial \xi}\xi_y+\frac{\partial \boldsymbol{F}_v}{\partial \eta}\eta_y=0 \tag{2}$$

The Jacobian matrix, $\boldsymbol{B}=\frac{\partial \boldsymbol{E}}{\partial \boldsymbol{U}}\eta_x+\frac{\partial \boldsymbol{F}}{\partial \boldsymbol{U}}\eta_y+\eta_t$,The characteristic field approaching the shock from behind correspond to the eigenvalue with a positive sign is $(u\eta_x+v\eta_y+\eta_t+c\sqrt{\eta_x^2+\eta_y^2})$. Where c is speed of the sound. The corresponding eigenvecter is $\boldsymbol{I}_L$. The compatibility relation immediately behind the shock can be obtained as

$$\boldsymbol{I}_L\cdot\left(\frac{\partial \boldsymbol{U}}{\partial \tau}+\left(\frac{\partial \boldsymbol{E}}{\partial \boldsymbol{U}}\eta_x+\frac{\partial \boldsymbol{F}}{\partial \boldsymbol{U}}\eta_y+\eta_t\right)\frac{\partial \boldsymbol{U}}{\partial \eta}+\frac{\partial \boldsymbol{E}}{\partial \xi}\xi_x+\frac{\partial \boldsymbol{F}}{\partial \xi}\xi_y+\frac{\partial \boldsymbol{U}}{\partial \xi}\xi_t+\frac{\partial \boldsymbol{E}_v}{\partial \xi}\xi_x+\frac{\partial \boldsymbol{E}_v}{\partial \eta}\eta_x+\frac{\partial \boldsymbol{F}_v}{\partial \xi}\xi_y+\frac{\partial \boldsymbol{F}_v}{\partial \eta}\eta_y\right)=0 \tag{3}$$

The unsteady flow is computed using moving grid method. The characteristic compatibility equations at boundary of bow shock are derived using non-conservation variable. The current approach avoids the computation of second derivative of geometric parameters for the shock front.

Numerical results

1. Receptivity to free-stream waves The unsteady flow solutions are obtained by imposing weak perturbation waves in a uniform flow in the free stream.: fast acoustic waves, slow acoustic waves, entropy waves, and vorticity waves. They can be written as:

$$\begin{bmatrix}u'\\v'\\p'\\d'\end{bmatrix}=\begin{bmatrix}\varepsilon\\0\\\varepsilon/M_\infty\\\varepsilon M_\infty\end{bmatrix}e^{i\left(kx-\frac{F\,\mathrm{Re}}{10^6}t\right)},\quad\begin{bmatrix}u'\\v'\\p'\\d'\end{bmatrix}=\begin{bmatrix}\varepsilon\\0\\-\varepsilon/M_\infty\\-\varepsilon M_\infty\end{bmatrix}e^{i\left(kx-\frac{F\,\mathrm{Re}}{10^6}t\right)},\quad\begin{bmatrix}u'\\v'\\p'\\d'\end{bmatrix}=\begin{bmatrix}0\\0\\0\\\varepsilon M_\infty\end{bmatrix}e^{i\left(kx-\frac{F\,\mathrm{Re}}{10^6}t\right)},\quad\begin{bmatrix}u'\\v'\\p'\\d'\end{bmatrix}=\begin{bmatrix}0\\\varepsilon\\0\\0\end{bmatrix}e^{i\left(kx-\frac{F\,\mathrm{Re}}{10^6}t\right)} \tag{4}$$

Where $\varepsilon=5\times10^{-4}$ is the wave amplitude, $k=15$ is the free-stream wavenumber, $F=2\,655$ is the forcing frequency of the free-stream acoustic wave, x is the location and t is time.

The angle of blunt cone is 10°. The flow conditions are $Ma=15, Re=6\,026.$, the wall temperature is constant $T_w=193\mathrm{K}$. The solutions present in this paper are resolved by 160×120 grids.

The wave fields are represented by perturbations of instantaneous flow variables with respect to the local steady base flow variables at the same location. $q'(x,y,t)=q(x,y,t)-Q(x,y)$, $q(x,y,t)$is the instantaneous perturbation obtained by an unsteady numerical simulation of the nonlinear Navier-Stokes equations, and $Q(x,y)$ is the steady mean flow obtained by a separate steady flow simulation. Fig 1 shows the contours of instantaneous perturbations of velocity along axis x, velocity along axis y, pressure and vorticity after the low field reaches a time-periodic state. The instantaneous contours show the interaction of the free-stream disturbances with the bow shock and the development of disturbance waves in the boundary layer on the surface, the waves patterns in outside the boundary layer and in inside the boundary layer are different. The waves in the boundary layer of velocitys in Fig 1 showed there are three wave modes of disturbance. The wave fields of pressure and vorticity showed acostic waves behind bow shock enter boundary layer and interact with the disturbance in boundary layer, the vorticity waves behind bow shock developed along bodys with fluids, and there are a boundary between disturbance waves in outside boundary layer and in inside boundary layer.

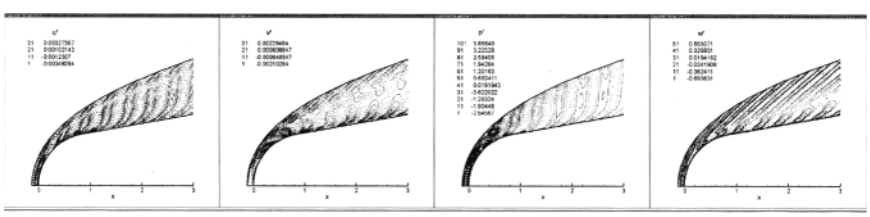

Fig1. Wave fields of velocity along axis x, y, pressure and vorticity

Kovasznay showed that weak disturbance waves in compressible flow can be decomposed into three independent modes: acoustic, entropy, and vorticity modes. The interaction of any kind of disturbances with a shock wave will produce three kinds of waves: acoustic, entropy, and vorticity waves. It is these disturbances generated behind the bow shock which propagate or convect downstream to enter the boundary layer.

Fig 2 shows a comparison of pressure, entropy, and vorticity perturbation amplitudes behind the bow shock generated by four kinds of incident waves in the free stream, fast acoustic waves slow acoustic waves entropy waves and vorticity waves. These wave amplitudes represent the strengths of acoustic, entropy and vorticity waves in the boundary.The results showed the receptivity in the boundary mainly is pressure disturbance, which represent acoustic waves, entropy waves and vorticity waves are weaker.

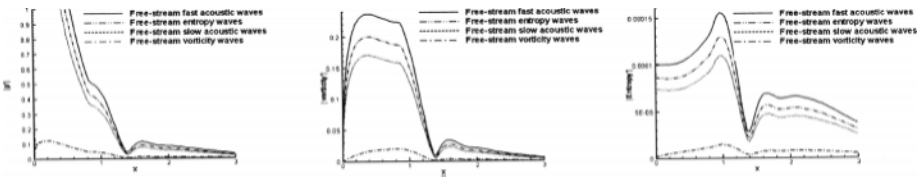

Fig2. Fourier amplitudes of the pressure, entropy, and vorticity in boundary layer

2. Wave modes in boundary layer Temporal Fourier analysis is carried out on the numerical solutions of perturbations of unsteady flow variables after a time-periodic state has been reached in a simulation.

$$q'(x,y,t) = Re\left(\sum_{n=0}^{N} |q'_n(x,y)|\, \mathrm{e}^{\mathrm{i}[-n\omega t+\phi_n(x,y)]}\right) \tag{5}$$

The Fourier amplitudes of pressure in the boundary layer for different frequencies are showed in Fig3. The amplitude for fundamental frequency is 10 times larger than the amplitude for second harmonic. The waves in the boundary layer mainly are fundamental mode(n=1).

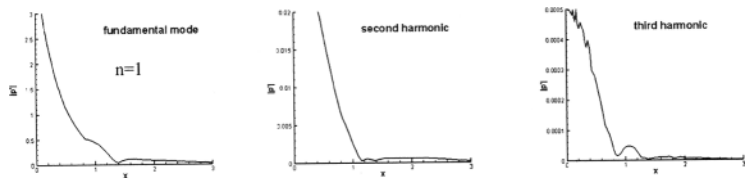

Fig3. Distribution of amplitudes of pressure perturbations in the boundary layer
(fundamental mode n=1,second harmonic n=2)

Mack difined the first, second, and third modes of a surpersonic boundary on a flat plate by the structure of the real part of the eigenfunctions of pressure perturbations. The nmber of zeros in the eigenfunctions was used by Mack to identify the mode number for compressible boundary layers. Fig 4 shows the variation of the real part of the Fourier transform for the pressure perturbations obtained by the numerical simulations in this paper. It shows the mainly wave modes in the boundary layer is frist mode near the head of the blunt cone and change to second and third modes at backward positions.

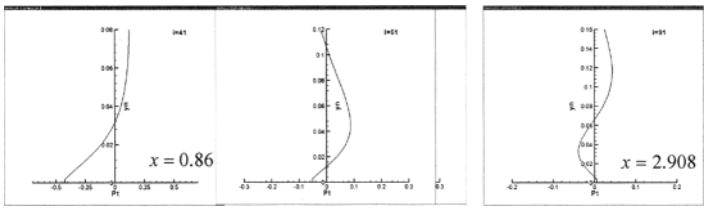

Fig4 Variation of the real part of the Fourier transform for the pressure perturbations along grid lines normal to the blunt cone surface at three grid stations

CONCLUSIONS

The result shows the high-order shock-fitting finite difference scheme in this paper is effective.

The effects of bow-shock and free-stream disturbance interactions are important for the receptivity process of hypersonic flow. The acoustic waves generated at the bow shock are mainly responsible for generating hypersonic boundary layer instabilities.

In the blunt cone hypersonic boundary layers, the acoustic disturbance is stronger than entropy disturbance and vorticity disturbance.

On the body surface, first, second, and even higher modes are generated and propagate downstream along the wall. The first mode increases first and then decreases, after the first mode decay, the second and third mode disturbance become dominant.

Acknowledgements

The support of China Natural Science Foundation under 10502052 is gratefully acknowledged.

REFERENCES

1. Fu DMa Y WLiu H. Upwind compact scheme and application. In: Proceedings of the 5^{th} International Symposium on Computational Fluid Dynamics, 1993; **1**: 184-190
2. Reshotko E. Hypersonic stability and transition. In: Hypersonic Flows for Reentry Problems, vol.1(ed. J.-A. Desideri, R. Glowinski & J. Periaux), 1991; 18-34
3. Zhong X L. Leading-edge receptivity to free-stream disturbance waves for hypersonic flow over a parabola. *J Fluid Mech*, 2001; **441**: 315-367
4. Ma Y B, Zhong X L. Receptivity of a supersonic boundary layer over a flat plate. Part 1: Wave structures and interactions. *J Fluid Mech*, 2003; **488**: 31-78
5. Ma Y B, Zhong X L. Receptivity of a supersonic boundary layer over a flat plate. Part 2: Receptivity tofree-stream sound. *J Fluid Mech*, 2003; **488**: 79-121
6. Kovasznay L S G. Turbulence in supersonic flow. *J Aero Sci*, 1953; **20**: 657-682